(5) J. Sohma, S. Shimokawa, and K. Hotta, "Recent Development of Magnetic Resonance in Biological Systems", S. Fujiwara and L. H. Piette, Ed., Hirokawa Publishing Co., Tokyo, Japan, 1968, p 57.
(6) T. Yokono, S. Shimokawa, H. Fukui, and J. Sohma, *Nippon Kagaku Zasshi*, **2**, 201 (1973).
(7) S. Shimokawa, H. Fukui, J. Sohma, and K. Hotta, *J. Am. Chem. Soc.*, **95**, 1777 (1973).
(8) L. S. Kan and N. C. Li, *J. Am. Chem. Soc.*, **92**, 4823 (1970).
(9) F. Jordan and B. Y. McFarquhar, *J. Am. Chem. Soc.*, **94**, 6557 (1972).
(10) J. A. Happe and M. Morales, *J. Am. Chem. Soc.*, **88**, 2077 (1966).
(11) S. M. Wang and N. C. Li, *J. Am. Chem. Soc.*, **90**, 5069 (1968).
(12) L. S. Kan and N. C. Li, *J. Am. Chem. Soc.*, **92**, 281 (1970).
(13) T. Yokono, S. Shimokawa, and J. Sohma, *J. Am. Chem. Soc.*, **97**, 3827 (1975).
(14) C. H. Chang and L. G. Marzilli, *J. Am. Chem. Soc.*, **96**, 3656 (1974).
(15) L. Sillén, Ed., *Chem. Soc. Spec. Publ.*, **No. 17** (1964).
(16) N. A. Rambaut and H. L. Peeters, *Bull. Soc. Chim. Belg.*, **76**, 33 (1967).
(17) D. C. Luehrs and K. Abate, *J. Inorg. Nucl. Chem.*, **30**, 549 (1968).
(18) J. S. Dunnett and R. P. H. Gasser, *Trans. Faraday Soc.*, **61**, 922 (1965).
(19) U. P. Strauss, C. Helfgott, and H. Pink, *J. Phys. Chem.*, **71**, 2550 (1967).
(20) H. G. Hertz, *Z. Elektrochem.*, **65**, 36 (1961).
(21) T. R. Stengle and J. D. Baldeschwieler, *Proc. Natl. Acad. Sci. U.S.A.*, **55**, 1020 (1966).
(22) R. P. Haugland, L. Stryer, T. R. Stengle, and J. D. Baldeschwieler, *Biochemistry*, **6**, 498 (1967).
(23) G. Gillberg-LaForce and S. Forsen, *Biochem. Biophys. Res. Commun.*, **38**, 137 (1970).
(24) M. Zeppezauer, B. Lindman, S. Forsen, and I. Lindqvist, *Biochem. Biophys. Res. Commun.*, **37**, 137 (1969).
(25) J. L. Sudmeier and J. J. Pesek, *Anal. Biochem.*, **41**, 39 (1971).
(26) R. G. Bryant, *J. Am. Chem. Soc.*, **91**, 976 (1969).
(27) R. G. Bryant, *J. Am. Chem. Soc.*, **89**, 2496 (1967).
(28) H. Csopak, B. Lindman, and H. Lilja, *FEBS Lett.*, **9**, 189 (1970).
(29) A. G. Marshall, *Biochemistry* **7**, 2450 (1968).
(30) C. F. Springgate, A. S. Mildvan, R. Abramson, J. L. Engle, and L. A. Loeb, *J. Biol. Chem.*, **248**, 5987 (1973).
(31) W. D. Ellis, H. B. Dunford, and J. S. Martin, *Can. J. Biochem.*, **47**, 157 (1969).
(32) R. G. Bryant, *Biochem. Biophys. Res. Commun.*, **37**, 603 (1969).
(33) T. R. Collins, Z. Starcuk, A. H. Burr, and E. J. Wells, *J. Am. Chem. Soc.*, **95**, 1649 (1973).
(34) A. Abragam, "The Principles of Nuclear Magnetism", Oxford, London, 1961, p 314.
(35) K. J. Johnson, J. P. Hunt, and H. W. Dodgen, *J. Chem. Phys.*, **51**, 4493 (1969).
(36) H. G. Hertz and M. Holz, *J. Phys. Chem.*, **78**, 1002 (1974).
(37) R. R. Sharp, *J. Chem. Phys.*, **57**, 5322 (1972).
(38) R. M. Hawk, R. R. Sharp, and J. W. Tolan, *Rev. Sci. Instrum.*, **45**, 96 (1974).
(39) R. R. Sharp and J. W. Tolan, *J. Chem. Phys.*, in press.
(40) J. A. Pople, W. G. Schneider, and H. J. Bernstein, "High Resolution Nuclear Magnetic Resonance", McGraw-Hill, New York, N.Y., 1959, Chapter 10.
(41) S. Kang, *Jerusalem Symp. Quantum Chem. Biochem.*, **5**, 271 (1973).
(42) C. W. Davies, "Ion Association", Butterworths, Washington, D.C., 1962, Chapter 3.

Molecular Rydberg Transitions. 3. A Linear Combination of Rydberg Orbitals (LCRO) Model for the Two-Chromophoric System 2,2,4,4-Tetramethylcyclobutane-1,3-dione (TMCBD)[1]

P. Brint, K. Wittel, P. Hochmann, W. S. Felps, and S. P. McGlynn*

Contribution from the Coates Chemical Laboratories, The Louisiana State University, Baton Rouge, Louisiana 70803. *Received March 19, 1976*

Abstract: The Rydberg absorption spectra of acetone and 2,2,4,4-tetramethylcyclobutane-1,3-dione (TMCBD) have been obtained and analyzed. TMCBD is treated as a composite of two acetone molecules and its Rydberg spectrum is analyzed by comparison with that of acetone. In order to retain the categorization of molecular Rydberg levels as s, p, d, . . . (or, equivalently, to retain the assignment power of empirical quantum defect ranges), we are forced to develop a linear combination of Rydberg orbitals (LCRO) model. The LCRO model leads to a facile analysis of the TMCBD spectrum, whereas a one-center model, in which the Rydberg orbital is positioned on the inversion center of TMCBD, does not. The implications of the LCRO model with respect to Rydberg intensities, precursor orthogonality requirements, charge delocalization in Rydberg states, the completeness or incompleteness of Rydberg series, and the empirical content of the s, p, d, . . . labeling are discussed briefly.

Introduction

A major goal of molecular spectroscopy is the transcription of chemical relatedness onto the spectroscopic data. An outstanding example of this approach is furnished by photoelectron spectroscopy, where a large amount of data (i.e., ionization potentials) has been correlated by using the molecular orbital approximation in varying degrees of sophistication.[2] The MO method, bolstered, as required, by configuration interaction, can also account for most of the valence excitations observed in electronic spectroscopy. Extravalence or "Rydberg" excitations, on the other hand, have been discussed, almost exclusively on the basis of the Rydberg equation

$$h\nu = I - [R/(n + \delta)^2] \qquad (1)$$

where $h\nu$ is the energy of the Rydberg transition; I is the ionization energy to which the Rydberg series of interest converges; R is the Rydberg constant; δ is the so-called quantum defect; and n is a serial index, $n = 1, 2, 3, \ldots$, which identifies individual members of a given series. This equation has been used mostly for correlating different electronic transitions within one atom or molecule.[3a] Recently, however, eq 1 has also been applied to the correlation of related transitions within different molecules.[3]

The present work represents an attempt to carry the idea of intermolecular correlation somewhat further. Specifically, we view 2,2,4,4-tetramethylcyclobutane-1,3-dione (TMCBD) as a composite of two acetone moieties and attempt an interpretation of the vacuum uv spectrum of the former by exploiting fully the knowledge available for the vacuum uv spectrum of the latter. Although this approach is not totally alien to vacuum uv spectroscopy,[4,5] it does seem appropriate to review some traditional ideas about Rydberg states before presentation of the model.

Acetone and TMCBD are shown in Figure 1. If acetone be denoted A, it does not seem inappropriate to denote TMCBD as A_LA_R, where the subscripts L/R denote left/right, respectively. If the association $A \leftrightarrow A_LA_R$ is a valid one with respect to the acetone $\leftrightarrow$ TMCBD dyad, it follows that the vacuum uv spectrum of TMCBD should exhibit some sort of

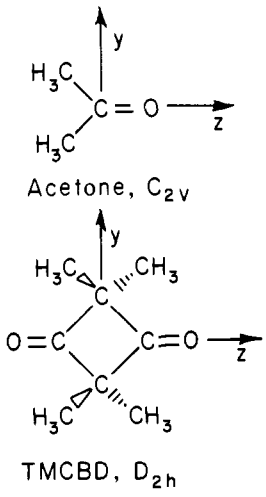

Figure 1. The molecules acetone and 2,2,4,4-tetramethylcyclobutane-1,3-dione (TMCBD).

relationship to that of acetone. Hence, the plan of our article is straightforward. It consists, in succession, of a short discussion of Rydberg ideas, the presentation of a model for the interaction of two identical Rydberg systems, the experimental aspects of the vacuum uv spectra of acetone and TMCBD and their analysis using the Rydberg equation and our model, and, finally, the implications of this model and its relationship to traditional concepts.

Rydberg Orbitals.[6] Rydberg states are "states in which one electron is excited to an [atomic] orbital large in size compared with a "core" [which is usually singly charged]".[7] For atoms, eq 1 is found to be the exact solution for the simple potential[8]

$$V(r) = (-1/r) + (M/r^2) \tag{2}$$

Since eq 1 is also obeyed by molecular Rydberg states, one must suppose that the corresponding Rydberg orbitals also retain a considerable degree of atomic character. Indeed, with the supposition that the Rydberg [molecular] orbital is large—a supposition which must be true[7] for large n—the details of the molecular core will introduce only a minor perturbation and the labels s, p, d, . . . will retain physical meaning, exactly as in the atomic case.

In linear molecules, the p-orbital manifold will split into $p\sigma$ and $p\pi$ components and, in molecules of lower symmetry, into components which transform as the relevant irreducible representations. Such splitting implies a degeneration of the physical content of the labels s, p, d, ... Furthermore, even though a complete analysis may be feasible on the basis of detailed studies of certain linear molecules,[9] the assignment tactic for polyatomics usually depends[3a] on the value found for the quantum defect, δ, of eq 1. The s, p, d, . . . nature of the Rydberg orbital is inferred from the value of δ. This may or may not be a valid practice. Certainly, it is a very heavily used practice and we will use it also. In any event, what we stress is that the s, p, d, . . . labels for polyatomics are usually imposed and not deduced and that the validity of these labels, particularly for low n, is open to serious question.

Linear Combination of Rydberg Oribtals (LCRO). We wish to relate the Rydberg orbitals of a composite molecule A_LA_R to those of two (identical) parts A. We will use an orbital picture and we start from the knowledge of the orbitals φ^c and φ^R, which serve to describe the transition $\varphi^c \rightarrow \varphi^R$ in the parent system A. The superscripts "c" and "R" denote core and Rydberg orbitals, respectively. As orbitals pertinent for the composite molecule, A_LA_R, we take the linear combinations

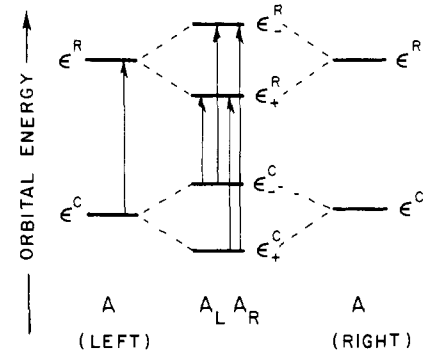

Figure 2. Splitting of valence and Rydberg orbitals in a composite molecule which contains two identical R chromophores. The order of orbitals is the "natural order" (i.e., $\epsilon_- > \epsilon_+$). The order which occurs in a given molecule must be determined by experiment. In TMCBD, for example, it is found that[10,11] $\epsilon_-{}^c < \epsilon_+{}^c$, in contradistinction to the above diagram.

$$\begin{aligned}
\varphi_+{}^c &= [2(1 + S^c)]^{-1/2}(\varphi_L{}^c + \varphi_R{}^c) \\
\varphi_-{}^c &= [2(1 - S^c)]^{-1/2}(\varphi_L{}^c - \varphi_R{}^c) \\
\varphi_+{}^R &= [2(1 + S^R)]^{-1/2}(\varphi_L{}^R + \varphi_R{}^R) \\
\varphi_-{}^R &= [2(1 - S^R)]^{-1/2}(\Phi_L{}^R - \varphi_R{}^R)
\end{aligned} \tag{3}$$

where

$$S^c \equiv \langle \varphi_L{}^c | \varphi_R{}^c \rangle; S^R \equiv \langle \varphi_L{}^R | \varphi_R{}^R \rangle$$

Because of various interactions, the orbital energies $\varphi_{+/-}{}^c$ and $\varphi_{+/-}{}^R$ will exhibit some displacement from those of the parent orbitals φ^c and φ^R, respectively. The resultant splitting is depicted schematically in Figure 2. Four different R ← N transitions of A_LA_R, $\varphi_\pm{}^c \rightarrow \varphi_\pm{}^R$, are now predicted to replace each of the $\varphi^c \rightarrow \varphi^R$ transitions of A.

This model, which is familiar for valence orbitals, appears to be a quite natural extension for Rydberg orbitals also. However, the LCRO MO idea is directly opposed to the concept of an atomic-like Rydberg orbital, which ought to be readily and accurately representable by a one-center function or functions[12] and which should be classifiable on an l quantum number basis. We will return to the contradictions between the LCRO model and certain common attitudes about Rydberg orbitals later, but only after a more thorough exposition of this LCRO model.

Requirements for Test Molecules. In the final analysis, the LCRO model must be tested using specific molecules A and A_LA_R. The requirements to be imposed on these two molecular systems are:

(a) The energy gap between the highest energy filled MO, φ^c, of A and the more tightly bound core MO's of A must be reasonably large. This requirement ensures a large energy gap, and a minimal configuration mixing, between the lowest energy Rydberg members which initiate in φ^c and those which initiate in the more tightly bound MO's. This energy gap is ~2 eV in acetone[13] and is adequately large for our purposes.

(b) A reasonably secure analysis of the Rydberg systems of A must be either available or feasible. Requirement a above ensures a certain simplicity of the Rydberg spectrum of A and the possibility of a ready analysis.

(c) The splitting of the valence orbitals, $\varphi_+{}^c$ and $\varphi_-{}^c$, of A_LA_R must be large enough in order to avoid extensive overlapping and mixing of the Rydberg states which arise from $\varphi_+{}^c$ and $\varphi_-{}^c$ excitations. This splitting in TMCBD is only 0.73 eV,[10,11] which is somewhat less than desirable. For example, this 0.73-eV difference translates into a spectroscopic gap of ~180 Å between the first p_y Rydberg members which initiate in $\varphi_+{}^c$ and $\varphi_-{}^c$ excitations in TMCBD. Requirement a for A must also apply to A_LA_R, except that now we require a large

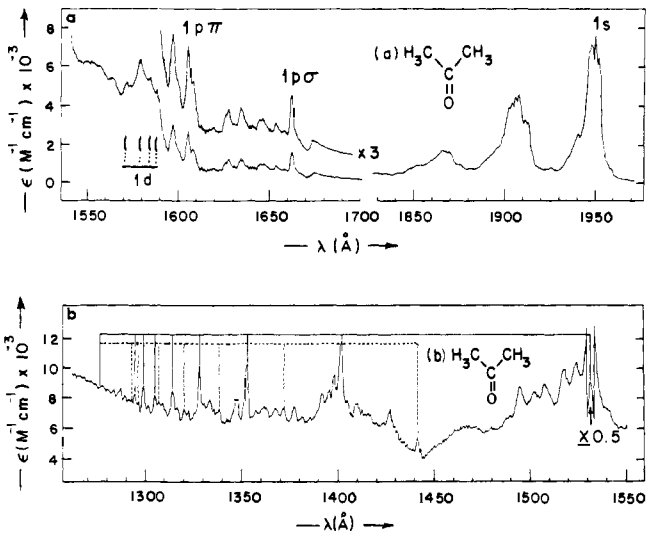

Figure 3. (a) The absorption spectrum of acetone in the 1970–1550-Å region. No significant absorption is detected between 1700 and 1830 Å. Refer to Table I for band identifications. (b) The absorption spectrum of acetone in the 1550–1270-Å region. Solid vertical lines denote s Rydberg series members for $n \geq 2$; dashed vertical lines denote pσ Rydberg series members for $n \geq 2$. Refer to Table I for further details.

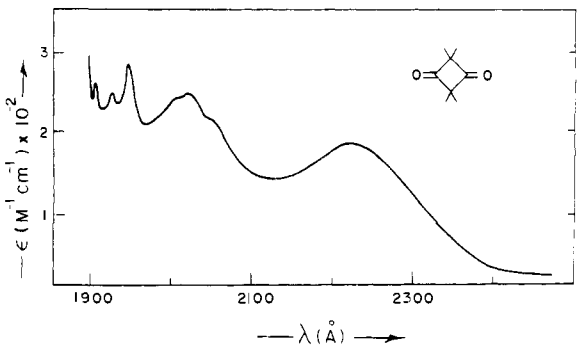

Figure 4. The absorption spectrum of 2,2,4,4-tetramethylcyclobutane-1,3-dione in the 2400–1900-Å region. Refer to Table II for further details.

gap between the topmost filled MO of A_LA_R (whether φ_+^c or φ_-^c is irrelevant) and the subjacent core σ MO's. This gap, for TMCBD,[10,11] is also ~2 eV.

(d) The photoelectron spectrum of A_LA_R must exhibit a lowest energy ionization event which is sharp and which may or may not be vibronically structured. It is known[3a] that the photoelectron band structure associated with the ionization event $I(\varphi_j^c)$ is largely replicated in the Rydberg spectrum generated by excitation of an electron from the φ_j^c MO. This requirement is pertinent to the observability of low-energy Rydbergs in A_LA_R and, when observed, it facilitates their assignment. This requirement is satisfied by TMCBD.[11] It should also be satisfied by A and is, for A ≡ acetone.[13]

(e) A_LA_R should, if possible, be centrosymmetric. This high symmetry introduces gerade/ungerade (g/u) selection rules. Thus, if φ_+^c is of u-type, R ← N transitions which initiate in φ_+^c are allowed only when the terminal (i.e., Rydberg) orbital is of g-type. TMCBD possesses an appropriate symmetry, being D_{2h} in its ground state.[14,15] In addition, it is known that the topmost filled MO of TMCBD is of u-type[10,11] (i.e., φ_+^c). Thus, in a one-center description of the Rydberg orbitals of TMCBD—such orbitals, of necessity, being located at the center of the cyclobutane ring—the transitions $\varphi_+^c \rightarrow ns$ and $\varphi_+^c \rightarrow nd$ are allowed, whereas transitions $\varphi_+^c \rightarrow np$ are forbidden. Consequently, the observation of a strong transition of $\varphi_+^c \rightarrow np$ type in TMCBD is an adequate reason for rejection of the one-center description of Rydberg orbitals in this system.

(f) The A_LA_R system must be reasonably rigid. Unfortunately, cyclobutane systems are not noted for their rigidity. Furthermore, it is well known that the excitation of the nonbonding electron of a carbonyl group tends to destroy planarity of the carbonyl group and its attachments. Thus, formaldehyde is planar in its ground state, but pyramidal in its $^1\Gamma_{n\pi^*}$ state.[16] Indeed, TMCBD is found to be nonplanar in certain of its four low-energy $^1\Gamma_{n\pi^*}$ states.[17,18] Such an induction of nonplanarity may destroy centrosymmetric character and it may invalidate the arguments embodied in e above. In any event, such nonplanarity, if it occurs in Rydberg states, may be detected by vibrational analysis. Considerable vibronic activity in either skeletal bending modes or carbonyl wagging modes should be evident if the cyclobutane system bends or the carbonyl system goes pyramidal, respectively.

(g) Both the A and A_LA_R systems must be stable. It is this requirement which dictates the presence of the four methyl attachments of TMCBD. Both acetone and TMCBD are adequately stable for the purposes of this work, but only if investigated under continuous-flow conditions (see Experimental Section).

(h) The separation of the two chromophoric systems, one on A_L and one on A_R, must be neither too small nor too large. If too small, the orbital on the right segment may become linearly dependent on the one on the left segment (vide infra); and, if too large, the two orbitals may not interact at all and A_LA_R may behave simply as a "double A" system. The rationale for these restrictions will be discussed later. For now, let it suffice that an interchromophoric distance of ~4 Å, such as is found in TMCBD, appears to be of the appropriate size.

Experimental Section

Vapor spectra in the vacuum uv region were recorded under continuous gas-flow conditions on a McPherson 225 1-m dual path spectrometer. The grating was blazed at 1200 Å and contained 1200 lines/mm. The reciprocal linear dispersion was 8.3 Å/mm. The light source was a Hinteregger, hydrogen discharge lamp which, via a cam-driven sliding plunger, was operated in a windowless mode. Monochromator slit widths varied from 40 to 70 μm and corresponded to band-pass extents of 0.6–1.1 Å. The absorbing path length was 10 cm and the cell temperature was controllable to within ±1 °C. Unless otherwise stated, all vacuum uv spectra were obtained at 22 °C.

Vacuum uv spectra were recorded prior to and after outgassing of the samples. No spectral differences were noted, nor was any evidence of photodecomposition observed under minimal flow conditions.

The 1 s feature of acetone in the 1950–1850 Å region was also studied under static conditions at 0.3 Å resolution on a modified Cary 15 spectrophotometer. The resolution obtained was a function of time. The extremely sharp fine structure observed at $t \simeq 0$ was gradually obliterated over a period of ~15-min exposure to the dispersed excitation beam of the D_2 lamp at 1950 Å. Photoreactions were presumed to be occurring. These photoreactions were eliminated by the simple expedient of continuously flowing the vapor through the absorption cell and were not studied further. However, this observation indicates that all static measurements of the acetone spectrum should be treated with some caution. It is also of note that the acetone spectrum in this region contains considerably higher resolution than displayed in the McPherson recording of Figure 3, where the band pass was ~1 Å.

The low-energy, 1850–2300 Å, absorption region of TMCBD was recorded on a purged Cary 15 spectrophotometer. The cell length was 10 cm. The cell temperature was varied between 60 and 100 °C and was maintained constant within ±2 °C during any one run. The cell, plus TMBCD, was outgassed at 22 °C and 10^{-3} mm prior to all spectroscopic measurements. All measurements were static (i.e., zero gas flow). No photodecomposition was noted in this work, though there are reports of such in the literature.[19] The low-energy spectrum of TMCBD is presented in Figure 4. The vacuum uv spectrum of TMCBD is given in Figure 5.

Photoelectron spectra were recorded on a Perkin-Elmer PS-18

spectrometer. Acetone vapor was introduced directly into the ionization chamber. A heated probe operated at 60 °C was used to generate TMCBD vapor from a solid ampule situated in the ionization chamber. Spectra were calibrated using Ar and Xe $^2P_{1/2}$ and $^2P_{3/2}$ lines. The resolution was typically 25 meV.

The acetone was a fluorometric grade sample and, apart from drying and outgassing, was used as received. TMCBD (Aldrich) was purified by repeated recrystallization from benzene, followed by a three-stage vacuum sublimation.

Extinction coefficients, where shown, were estimated from the measured vapor pressures. However, since the majority of all optical measurements were carried out on flowing systems, and since pressures were measured only at the inlet and outlet ports of the cell, it is possible that the absolute extinction coefficients may be in error by ±50%. However, all extinctions internal to the total spectrum of any one molecule should be relatively correct to ±5%.

Results

Acetone. The vacuum uv spectrum of acetone is shown in Figure 3 (a and b). This spectrum has been the object of a number of investigations.[20-22] The most informative optical study is due to Watanabe,[21] who assigned one Rydberg series and commented on the probable existence of others. He also suggested that the 1950-Å band, which had previously been thought to be a valence excitation of n → σ* type, should be reassigned as a Rydberg transition. The most detailed electron energy loss study is due to Huebner, Celotta, Mielczarek and Kuyatt.[20] These authors assigned three Rydberg series and much of the vibronic details. In addition, they provided[20] an admirable summary of the existing literature on the vacuum uv spectrum of acetone, and repetition here would be superfluous.

The resolution intrinsic to Figure 3 is somewhat higher than that of previous authors. Nonetheless, the agreement with previous authors, particularly Huebner et al.,[20] is extensive. Hence, our discussion of the acetone spectrum will be terse and will only touch on the major areas of agreement, the few areas of disagreement being emphasized.

The acetone spectrum consists of a number of Rydberg series, all of which converge to the first ionization potential, I_1. Three distinct types of series are observed. In each of these, the quantum defect, $\delta_{n\alpha}$, tends toward a constant value as n increases. The quantities n and $\delta_{n\alpha}$ are defined in terms of eq 1, E and δ being replaced by $E_{n\alpha}$ and $\delta_{n\alpha}$, respectively. The value of I_1 is found to be 78 350 cm^{-1} (9.714 eV). The limiting values of the quantum defect, $\lim_{n\to\infty}\delta_{n\alpha} \equiv \delta_\alpha$, for the four observed series are:

$$\delta_s = 0.97, \text{ s-type series}$$

$$\delta_{p\sigma} = 1.48, \text{ p-type series}$$

$$\delta_{p\pi} = 1.62, \text{ p-type series}$$

$$\delta_d = 1.71, \text{ d-type series}$$

The designations of molecular Rydberg series in terms of an atomic orbital angular momentum l follows by comparison with the values of δ_l for atomic systems. For example, δ_s = 0.84, δ_p = 1.32, and δ_d = 1.75 for the rare gases. The pσ/pπ subclassification is based on Lindholm's analysis of linear molecules.[23] Values of n and $\delta_{n\alpha}$ for individual members of the various series are listed in Table I. We will now discuss the individual series.

s Series. This series consists of a progression of single electronic origins. These are the most intense features throughout the spectrum. This series is identical with that of Watanabe[21] and Huebner et al.[20] The value of δ_{1s} is anomalously high; however, abnormalities of δ are a common property of lowest energy Rydberg bands of s type.[3a]

p Series. For $n < 6$, two p origins are observed. For $n > 6$, both p origins are unresolved; the peaks of the resulting band envelopes are best assigned to the lower energy series because of the retention of quantum defect similarities.

The pσ series appears to correspond to Huebner's "series II". The differences of apparent resolution between the two spectra make any further correspondence difficult to establish. We find that the p series converges smoothly on I_1.

d Series. A number of electronic origins are bunched together in the 1570-1590-Å region. Five "apparent" origins are listed in Table I; however, the number of "true" origins is probably less than this. In any event, it is clear that the 1570-1590-Å band envelope contains the first members of several similar Rydberg series, all of which are assigned as d-Rydberg series. Due to the energy proximity of these first members, the individual d series converge rapidly on one another with increasing n. As a result, some of the peaks which were resolved for n = 1 grow indistinct for $n \geq 2$ and merge into a single, broad, band envelope for $n \geq 5$.

The d series exhibits good correspondence with Huebner's

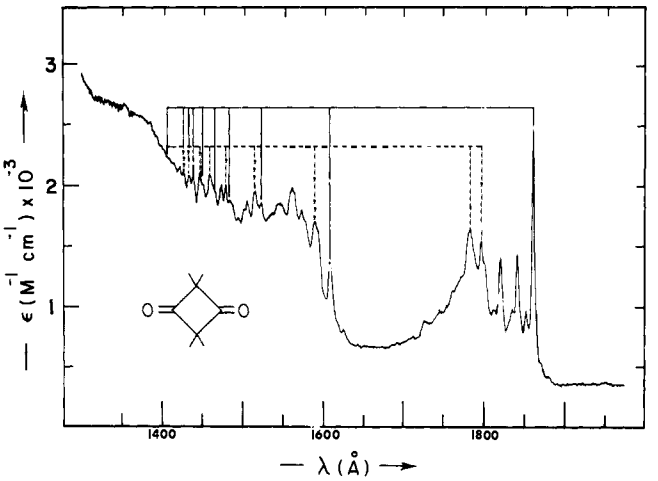

Figure 5. The absorption spectrum of 2,2,4,4-tetramethylcyclobutane-1,3-dione in the 1950-1350-Å region. Solid vertical lines denote the p-series members and dashed vertical lines denote the d-series members. Refer to Tables II and III for further details.

Table I. Wavelengths (Å), Serial Indices (n), and Quantum Defects ($\delta_{n\alpha}$) for the Rydberg Transitions of Acetone [I_1 = 78 350 cm^{-1}]

s Series			pσ Series			pπ Series		
λ_{ns}	n	δ_{ns}	$\lambda_{np\sigma}$	n	$\delta_{np\sigma}$	$\lambda_{np\pi}$	n	$\delta_{np\pi}$
1950.0	1	1.01	1662.6	1	1.46	1606.0	1	1.61
1531.0	2	0.90	1441.0	2	1.50	1427.0	2	1.64
1402.0	3	0.95	1372.0	3	1.48	1365.5	3	1.63
1353.0	4	0.97	1338.5	4	1.49	1336.0	4	1.60
1328.0	5	1.00	1320.0	5	1.51	1318.5	5	1.62
1314.0	6	0.99	1309.0	6	1.49	1308.0	6	1.60
1305.0	7	0.98	1301.5	7	1.51			
1299.0	8	0.96	1296.5	8	1.49			
1294.5	9	0.99	1293.0	9	1.42			
1291.5	10	0.92						

d Series								
λ_{nd}	n	δ_{nd}	λ_{nd}	n	δ_{nd}	λ_{nd}	n	δ_{nd}
1589.0	1	1.67	1423.5	2	1.68	1334.5	4	1.67
1585.0	1	1.68	1419.5	2	1.73	1334.0	4	1.69
1579.5	1	1.70	1418.5	2	1.74	1333.0	4	1.74
1578.5	1	1.70	1363.0	3	1.69	1317.5	5	1.69
1572.0	1	1.73	1362.0	3	1.72	1307.0	6	1.71
			1360.0	3	1.77			

Table II. Vibrational Analysis of the First Photoelectron Band and of Several Rydberg Bands of TMCBD

	$\varphi_+^c \rightarrow 1s$		$\varphi_+^c \rightarrow 1p_z$		$\varphi_+^c \rightarrow 1p_y$		$\varphi_+^c \rightarrow 2p_y$		$\varphi_+^c \rightarrow 1d$		$I(\varphi_+^c)$	
Assignment	λ, Å	$\Delta\nu$, cm^{-1}	λ, Å	$\Delta\nu$, cm^{-1}	λ, Å	$\Delta\nu$, cm^{-1}	λ, Å	$\Delta\nu$, cm^{-1}	λ, Å	$\Delta\nu$, cm^{-1}	I, eV	$\Delta\nu$, cm^{-1}
0,0	2050	0	1948	0	1860.5	0	1608.8	0	~1796.5	0	8.74_2	0
ν_1					1850.9	267						
ν_2	2028	530	1927	560	1840.8	564	1593.7	588	~1778.0	579	8.81_7	565
$\nu_1 + \nu_2$					1830.5	867					8.84_4	805
$2\nu_2$	2004	1120	1906	1130	1820.1	1182	1577.5	1232	~1760.0	1154	8.89_2	1210
$\nu_1 + 2\nu_2$					1811.8	1432						
$3\nu_2$					1800.5	1780	1564.5	1760	~1743.0	1710	8.96	1775

[a] The labeling of vibrational modes in column 1 is arbitrary. The data for the 2050 and 1948 Å origins are least certain because of the large half-band widths found in these spectral regions.

"series III".[20] The values of the quantum defects are similar and, like Huebner, we are unable to locate more than the initial five members of any one specific d series.

Vibrational Structure. The vibrational structure of the acetone spectrum is extremely rich. The 1s Rydberg transition exhibits vibrational structure[14,20] which is similar to that observed in the photoelectron spectrum[13] associated with the removal of an electron from the oxygen b_2 lone pair. The three most intense vibronic bands correspond to vibrational frequencies of approximately 650, 1030, and 1250 cm^{-1} and have been observed previously.[24] These frequencies, together with two others at 190 and 570 cm^{-1}, occur throughout the whole vacuum uv spectrum and account for nearly all of its observed vibrational content.

The activity of these five vibrational modes provides the rationale for the broad structureless feature which occurs in the 1540–1565-Å region. This region should contain many vibronic transitions based on as many as five 1d origins and involving at least four vibrational frequencies; as a result, this unresolved feature in this particular spectral region is quite expected.

The loss of apparent resolution at higher energies is probably due to the onset of series converging to the second ionization potential, I_2. The photoelectron value[13] of I_2 is ~11.8 eV. Consequently, the 1s Rydberg transition associated with the I_2 series limit should occur at ~1475 Å. If such transitions reproduce the band shape of the I_2 photoelectron event, they should provide a structureless, varying intensity, background absorption, with a concomitant loss of definition in those series which terminate on I_1.

Ionization Energy. The value I_1 = 78 350 ± 50 cm^{-1} obtained here from Rydberg series analysis should be compared with existing values of 78 280 (Rydberg series),[21] 78 160 ± 80 (photoionization),[21] and 78 420 (photoelectron).[13] The residual differences presumably refer to slight calibration errors.

2,2,4,4-Tetramethylcyclobutane-1,3-dione (TMCBD). The absorption spectra of the regions 2400–1900 and 1950–1350 Å are given in Figures 4 and 5, respectively. The 4000–2500-Å region contains four electronic transitions of $^1\Gamma_{n\pi^*} \leftarrow {}^1\Gamma_1$ (i.e., $n \rightarrow \pi^*$) type which have been the subject of considerable recent work.[17,18]

Several transitions in the 2400–1350-Å region exhibit vibrational structure. These structured bands are analyzed in Table II. The first photoelectron spectroscopic band, the I_1 band, exhibits vibrational structure and it is also analyzed in Table II. The vibrational modes, ν_1 and ν_2, of Table II may be identified as follows:[14]

ν_1: a_g skeletal bending; 293 cm^{-1} in $\tilde{X}\ {}^1A_g$

ν_2: a_g skeletal bending; 584 cm^{-1} in $\tilde{X}\ {}^1A_g$

The $3\nu_2$ identification is dubious; it could equally well be designated ν_3 and identified as the a_g symmetric carbonyl stretch which occurs[14] at 1851 cm^{-1} in $\tilde{X}\ {}^1A_g$. In any event, all of the observed structure is readily interpretable in terms of a_g vibronic activities. Hence, we may conclude two things: (i) since the origin bands of Table II are all fairly intense, the listed electronic transitions are electric-dipole allowed; and (ii) since the major vibrational activity is due to modes of a_g symmetry, no significant deviation from the ground-state symmetry occurs upon excitation. X-ray and electron diffraction data for the ground state of TMCBD[18] indicate a D_{2h} point group symmetry (exclusive of the methyl hydrogen atoms). Therefore, all the excited states listed in Table II must be essentially planar. This conclusion contrasts with those obtained from vibronic analyses of the *intravalence* $n \rightarrow \pi^*$ transitions where nontotally symmetric modes occur in prominent progressions and where, as a result, certain authors[17,18] conclude that the four $^1\Gamma_{n\pi^*}$ states may be of D_{2h}, C_{2v}, C_{2h}, or even C_s geometry. Such a conclusion, at least for the excited states listed in Table II, is unwarranted.

As indicated in Table II, a close similarity exists between the first photoelectron band and the 1860 Å absorption band. This similarity is demonstrated in Figure 6. The vibrational

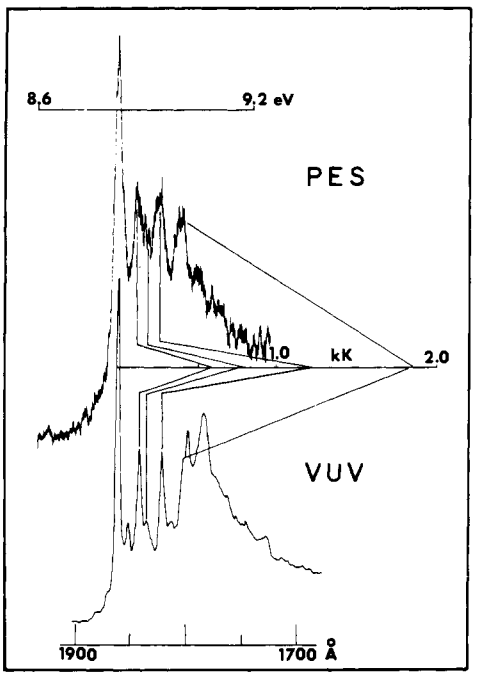

Figure 6. A comparison of the vibrational structure of the 1p Rydberg transition in 2,2,4,4-tetramethylcyclobutane-1,3-dione with that of the I_1 photoelectron band. The vibrational frequencies are compared on a kilokayser (1 kK = 10^3 cm^{-1}) scale.

Table III. Wavelengths (Å), Serial Indices (n), and Quantum Defects ($\delta_{n\alpha}$) for Rydberg Transitions Observed in the Spectrum of TMCBD [I_1 = 70 970 cm^{-1}]

s Series			p Series					
λ_{ns}	n	δ_{ns}	λ_{np_y}	n	δ_{np_y}	λ_{np_z}	n	δ_{np_z}
2050	1	1.22(?)	1860.5	1	1.52	1948	1	1.36
1743	2	0.84 ± 0.01	1608.8	2	1.53	1626	2	1.40
1561	3	0.99 ± 0.08	1523.5	3	1.54			
1507	4	0.88 ± 0.075	1484.5	4	1.52			
1475	5	0.88 ± 0.12	1462.5	5	1.50			
1457	6	0.85 ± 0.2	1449.0	6	1.49			

d Series			Band envelopes which consist of p and d components		
λ_{nd}	n	δ_{nd}	λ_{npd}	n	δ_{npd}
1796.5	1	1.68	~1440	7	1.48
1782.0	1	1.72	~1434	8	1.43
1589.2	2	1.69			
~1516.0	3	1.68			
~1480.0	4	1.68			
~1460.0	5	1.66			
~1447.0	6	1.68			

frequencies and Franck–Condon band shapes of both transitions are identical. Hence, the geometry of the cationic state and the upper state of the 1860-Å transition must be more or less identical and, as a result, we may conclude that the 1860-Å transition is a member of a Rydberg series which converges on I_1.

The analysis of the photoelectron spectrum of TMCBD[10,11] furnishes the ionization energies and the symmetries of the corresponding MO's which are listed in Figure 7. Using the ionization energy I_1 (b_{2u}), it is possible to assign virtually all nonvibrational vacuum uv features of the TMCBD spectrum to Rydberg series. These assignments are cited in Table III. A number of remarks concerning these assignments is in order.

Of the two, broad, lower energy transitions of Figure 4, one can be assigned as the first member of an s Rydberg series (i.e., as $\varphi_+^c \rightarrow 1s$). The effective quantum numbers of the higher energy members of this s series are n^* = 2.84, 3.98, 4.88, 5.88, 6.85, ... The maxima of the two transitions which lie at 2230 and 2050 Å correspond to n^* = 2.05 and 2.25, respectively, whereas the expected value is 1.9. The 2230-Å peak, therefore, is the preferred candidate (Table III). However, since low-energy Rydberg transitions usually deviate from the Rydberg equation,[3a] it is not proper to totally discard the 2025-Å assignment simply on the basis of its large effective quantum number. In fact, on the basis of the vibrational structure (Table II), it is the 2025-Å band, with origin at 2050 Å, which is the preferred candidate for the $\varphi_+^c \rightarrow 1s$ assignment.

The 2230-Å transition has been observed[25] previously in cyclohexane and ethanol solutions. It is also present in all solutions investigated in this work. This band exhibits little or no energy shifts in solvents of different polarity. The 2025-Å band is usually obscured because of absorption by the solvent medium, but is nonetheless observable in water, ether, and 3-methylpentane solutions. The disappearance or suppression of Rydberg transitions in fluid media is often supposed to be diagnostic for such transitions. However, in this instance, as well as in the majority of low-energy Rydberg transitions, these excitations may possess considerable intravalence character and need not exhibit any major intensity loss in condensed media.[3a] Hence, the insensitivity to solvent in this particular instance need not constitute evidence against a Rydberg assignment.

An earlier assignment of the 2230-Å band as an $n \rightarrow \sigma^*$ transition exists.[26] We find no basis on which to either agree or disagree with this assignment. We merely insist that some one of the 2230- and 2025-Å bands is of $\varphi_+^c \rightarrow 1s(R)$ type.

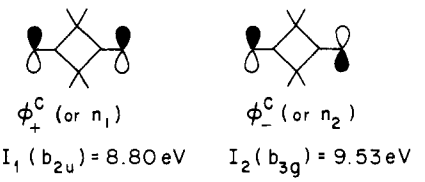

Figure 7. The two lowest energy ionization events in 2,2,4,4-tetramethylcyclobutane-1,3-dione. The core orbital which is depopulated in the cited ionization event is also schematized.

The 1948-Å origin is assigned as the $\varphi_+^c \rightarrow 1p_z$ Rydberg transition. The reasons for this assignment are threefold: First, the vibrational structure associated with this origin, as given in Table II, is similar to that found in the photoelectron band of Figure 6 and in the higher energy Rydberg transition of $\varphi_+^c \rightarrow 1p_y$ type. Thus, this transition is undoubtedly of Rydberg nature. Second, the effective quantum number of this origin is n^* = 2.36, in good accord with n^* = 3.40 for the other observed series member at 1626 Å. Third, the value of n^* = 2.36 is in reasonable agreement with the n^* = 2.46 for the $\varphi^c \rightarrow 1p\sigma$ transition of acetone, but not with the value n^* = 2.61 for the $\varphi^c \rightarrow 1p\pi$ transition of acetone.

The broadening of the higher energy absorption bands is caused by the onset of series which terminate on the third ionization limit, I_3. Such series should initiate at ~1600 Å and, since the I_3 photoelectron band is diffuse,[10,11] the same effects as those described previously for acetone may be expected for TMCBD for $\lambda \leq 1600$ Å. As a result, the intrinsic resolution of the TMCBD spectrum at high energies is much lower than that of acetone, and the series cannot be traced beyond n = 6 with any certainty.

A single s origin is found for n = 1, . . . , 6. However, the 1s origin, which lies at ~2200 Å, is of quite low intensity. Indeed, compared to acetone, the s series of TMCBD is radically changed. The bands of this series in TMCBD are broad, unresolved, and weak. Although intensity does increase with increasing n, the s series never attains the spectral dominance which it had in acetone. For this reason, band head measurements show rather large error margins for δ_{ns} (see Table III).

Table IV. Quantum Defects for the Rydberg Series of Acetone and TMCBD

Acetone	TMCBD
$\delta_s = 0.97$	$\delta_s \approx 0.89$ or 0.94
$\delta_{p\sigma} = 1.48$	$\delta_{p_z} = 1.38$
$\delta_{p\pi} = 1.62$	$\delta_{p_y} = 1.52$
$\delta_d \approx 1.71$	$\delta_d \approx 1.68$

An intense p origin is found for all np Rydberg transitions, $n = 1, \ldots, 6$. These transitions are assigned as $\varphi_+{}^c$ (b_{2u}) → np_y transitions.

Two 1d origins, $\delta_{1d} = 1.68$ and $\delta_{1d'} = 1.72$, occur. For $n \geq 2$, these two d origins have converged and occur as one band. For $n = 4$, 5, and 6, the p_y origins occur as shoulders on the slightly more intense d origins, but remain recognizable. For $n > 6$, p and d origins merge into a single band head and the ns bands are not observed.

Vala et al.[26] have reported the vacuum uv spectrum of TMCBD in the region 1900–1550 Å. Their spectrum agrees fully with the present work. Vala et al.[26] also performed CNDO/s, CNDO/2, and INDO calculations and, since they did not include diffuse orbitals in their basis sets, they assigned all observed bands to intravalance transitions. We do not concur with these assignments and prefer an *extravalence* set instead. In particular, on the basis of the Rydberg equation, photoelectron/vacuum uv band-shape similarities, quantum defect considerations, etc., we assign all but one electronic transition in the 2400–1400-Å region as $\varphi_+{}^c \rightarrow \varphi^R$ (i.e., as *extravalence*) transitions.

Discussion

The analysis of the vacuum uv spectrum of TMCBD yields several Rydberg series. The quantum defect values which characterize these series are compared with those for acetone in Table IV. We have used the standard correspondence[3a] between the atomic orbital angular momentum labels s, p, d, ... and certain ranges of quantum defect values in order to designate the various series as s, p, d, ... The σ/π or z/y subclassification of the p series is also based on quantum defect values and is in agreement with practices introduced by Lindholm[23] for small molecules.

The vibronic analyses of Table II indicate that TMCBD is centrosymmetric (D_{2h}) in various of its Rydberg (R) states. If we are to use a one-center description of Rydberg orbitals, symmetry adaptation requires that these Rydberg orbitals be situated on the center of symmetry. Since the highest energy occupied MO of TMCBD, $\varphi_+{}^c$ of Figure 7, transforms as b_{2u}, transitions to one-center Rydberg orbitals of p type (i.e., b_{1u}, b_{2u}, and b_{3u}) are parity forbidden, whereas those to Rydberg orbitals of s type (i.e., a_g) and d type (i.e., a_g, b_{1g}, b_{2g}, and b_{3g}) are parity allowed. Indeed, of all the parity-allowed transitions of d type, only one, namely that to the b_{2g} orbital, is symmetry forbidden.

If, alternatively, we describe the Rydberg orbitals of TMCBD as symmetry adapted, linear combinations of two carbonyl Rydberg orbitals, one from each of the two constituent carbonyl groups, we obtain a total of two s type, six p type, ten d type, ... Rydberg orbitals for each value of n. This two-center, LCRO model is schematized in Figure 8, where also is shown the polarization direction for allowed Rydberg transitions which initiate in $\varphi_+{}^c$ (b_{2u}).

The LCRO model provides the superior description of the observed Rydberg spectrum of TMCBD. This conclusion is based on the observation of electronically-allowed p-type Rydberg transitions in TMCBD; it is also independent of any estimates of orbital splittings and it evades all the pitfalls inherent in computations.[27]

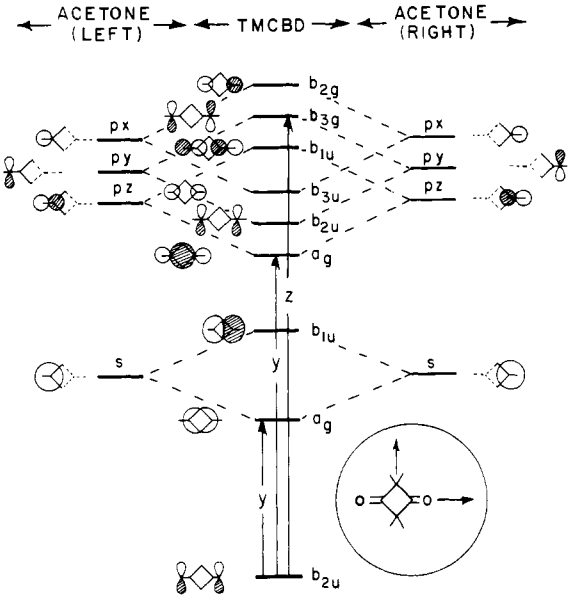

Figure 8. An LCRO model (schematic) for ns- and np-type Rydberg orbitals of TMCBD (center) as constructed from those of two acetone molecules, one right and one left. The extension to d-type Rydbergs is straightforward. Electric-dipole allowed transitions and their polarizations are also shown. Radial nodes in the p orbitals are not shown.

Finally, it must be admitted that the labels s, p, d, ... may not carry much meaning. It is only the symmetry designations appropriate for the particular molecular point group which have physical significance. Whether one or two center, the Rydberg orbitals have to transform as one of the irreducible representations. Thus the LCRO p-type Rydberg orbital of b_{3g} symmetry could equally well be considered to be of d type, to be single center, and to be located on the inversion center. The only observation which contradicts this latter (i.e., d type) supposition is that the value $\delta = 1.5$ for the np_y series of TMCBD is characteristic for p-type ($1.5 \leq \delta \leq 1.6$ in acetone) and not for d-type ($\delta = 1.72$ in acetone) transitions. In sum, if we wish to retain a quantum defect classification of molecular Rydberg states, we are forced into an LCRO model for TMCBD. The other alternative, namely rejection of the quantum defect classification, is unappealing in view of the analytic power intrinsic to this classification.[3a]

Given that the validity of an LCRO model has been established, this model has quite general consequences for Rydberg spectroscopy. We will now discuss some of these.

Number of Rydberg States. The LCRO model predicts twice the number of Rydberg states as does the conventional one-center, atom-like description. However, because of their large sizes, Rydberg orbitals which are located on different centers are expected and found[27] to have a large overlap—an overlap which may increase rapidly with increasing n. As a result, the two orbitals $\varphi_L{}^R$ and $\varphi_R{}^R$ may become linearly dependent and one may be expressed in terms of the other

$$\varphi_L{}^R = \langle \varphi_R{}^R | \varphi_L{}^R \rangle \cdot \varphi_R{}^R + \ldots . \quad (4)$$

$$\approx \langle \varphi_R{}^R | \varphi_L{}^R \rangle \cdot \varphi_R{}^R \quad (5)$$

The approximation of eq 5 tends toward an equality as the overlap integral tends toward unity. Thus, for large n, only one of the two linear combinations, $\varphi_{+/-}{}^R$ of eq 3, will survive and a one-center description will assuredly be more appropriate.[28] Viewed from a slightly different aspect, one of the linear combinations, $\varphi_{+/-}{}^R$ of eq 3, will finally become unbound for large n.

In a more specific vein, let us describe the Rydberg orbitals of a molecule A_LA_R by a set of Rydberg orbitals $\{\varphi_{Ln}{}^R, \varphi_{Rn}{}^R\}$

located, as indexed, on centers A_L and A_R. For large values of n, we expect large overlaps. Hence, we may write $\varphi_{Rn}{}^R$ in terms of $\varphi_{Ln}{}^R$ and a remainder ϕ_n, i.e.,

$$\varphi_{Rn}{}^R = S_n \cdot \varphi_{Ln}{}^R + (1 - S_n{}^2)^{1/2}\phi_n \tag{6}$$

where

$$\langle \varphi_{Ln}{}^R | \phi_n \rangle = 0;\ \langle \phi_n | \phi_n \rangle = 1;\ \text{and}\ S_n = \langle \varphi_{Ln}{}^R | \varphi_{Rn}{}^R \rangle$$

If we restrict interactions to orbitals with the same value of n and if we assume an identity of the two centers A_L and A_R, the orbital energies will be given by

$$\epsilon_{n\pm}{}^R = \frac{\langle \varphi_{Ln}{}^R | \mathrm{h} | \varphi_{Ln}{}^R \rangle \pm \langle \varphi_{Ln} | \mathrm{h} | \varphi_{Rn} \rangle}{1 \pm S_n} \tag{7}$$

where **h** is an appropriate, one-electron, effective Hamiltonian. Inserting $\varphi_{Rn}{}^R$ from eq 6 into eq 7 we obtain

$$\epsilon_{n\pm}{}^R = \langle \varphi_{Ln}{}^R | \mathbf{h} | \varphi_{Ln}{}^R \rangle \pm \langle \varphi_{Ln}{}^R | \mathrm{h} | \phi_n \rangle \cdot \left(\frac{1 - S_n}{1 + S_n}\right)^{\pm 1/2} \tag{8}$$

$$= \epsilon_n \pm \langle \varphi_{Ln}{}^R | \mathbf{h} | \phi_n \rangle \cdot \left(\frac{1 - S_n}{1 + S_n}\right)^{\pm 1/2} \tag{9}$$

The overlap-dependent term of eq 8 and 9 is shown in Figure 9 whence it is obvious that this term is not critical as long as $S_n \leq 0.8 \ldots 0.95$. In fact, since the magnitude of $\langle \varphi_{Ln}{}^R | \mathrm{h} | \phi_n \rangle$ may well decrease with increasing n, a fairly smooth behavior for both $\epsilon_{n-}{}^R$ and $\epsilon_{n+}{}^R$ can be expected. Eventually, the overlap term will dominate, and will produce an incomplete antibonding series. We are unable to decide the value of n for which the antibonding orbital will finally become unbound. This value of n, because of its dependence on overlap, will be a function of the separation of the two centers A_L and A_R. If this separation is adequately large, the movement of the antibonding LCRO virtual orbital into the continuum may well take place only when the energy differences between successive Rydberg series members of A (i.e., A_L or A_R) are already smaller than either rotational or vibrational quantum sizes—at which point the concept of an "electronic energy" has become meaningless anyway.

The above considerations are the basis for the requirement h, which was imposed in the Introduction, on the system A_LA_R. Unfortunately, knowing but little concerning the proper functional description of a Rydberg orbital of A, this requirement was, and remains, vague. In other words, our concerns with the magnitude of S_n suggest that the best chance for observation of both $\varphi_{n+}{}^R$ and $\varphi_{n-}{}^R$ for low values of n will occur when the interchromophoric distance is moderate (i.e., larger than that for a diatomic molecule, but small enough so that interactions do occur), hence, our choice of TMCB.

Meaning of the s, p, d, . . . Labels. As long as one retains the one-center description of Rydberg orbitals, the labels s, p, d, . . . carry the meaning of approximate quantum numbers and refer to orbital transformation properties under the operations of the spherical group. This meaning would seem to be totally lost in the LCRO description.

For polyatomics, the labels s, p, d, . . . characterize certain regions of quantum defect values: $\delta_s \sim 1.0$; $\delta_p \sim 1.4$; $\delta_d \sim 1.9$.[29] Now, the magnitude of the quantum defect is directly related to the degree to which the Rydberg orbital penetrates into the core or, equivalently, by the number of precursors which the Rydberg orbital possesses in the core. "Precursors" are core orbitals of the same symmetry as the Rydberg orbital in question or, alternatively, "precursors" are core orbitals with respect to which the Rydberg orbital has to be *radially* orthogonal. In atoms, and to some degree in diatomics, the number of precursors and, therefore, the extent of penetration

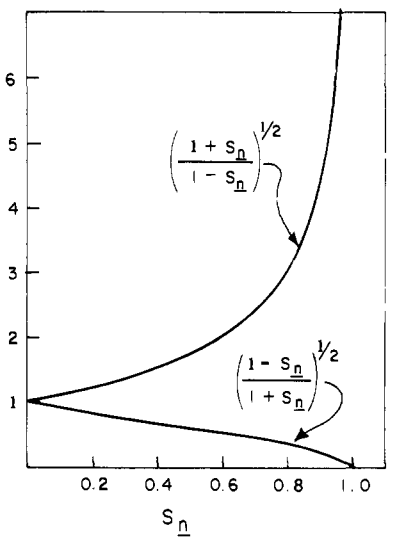

Figure 9. The influence of the overlap S_n on the splitting of Rydberg orbitals $\varphi_{\pm}{}^R$.

Table V. Precursors in TMCBD for Different Symmetry Species[a]

MO type	a_g	b_{1g}	b_{2g}	b_{3g}	b_{1u}	b_{2u}	b_{3u}	a_u
O, 1s	X				X			
C_{ring}, 1s	XX				X	X		
C_{methyl}, 1s	X	X				X	X	
O, 2s lone pairs				X		X		
σ, C=O	X				X			
O, 2s lone pair	X				X			
π, C=O			X				X	
Ring, σ(C-C)	X			X	X	X		
σ, C methyl	X	X				X	X	
σ, C-H	X	X				X	X	
σ, C-H	X	X				X	X	
σ, C-H			X	X	X			X
Total	10	4	2	3	6	7	5	1
AO's	s							
					p_z	p_y	p_x	
	d_{z^2}							
	$d_{x^2-y^2}$	d_{xy}	d_{zx}	d_{yz}				

[a] For LCRO representations, see Figure 8.

grows larger in the order d < p < s, leading one to expect $\delta_s < \delta_p < \delta_d$. For the neon atom, for instance, there are two s precursors (1s and 2s), one p precursor (2p), and no d precursors. This simple relationship does not exist in a large molecule such as TMCBD. The number of real precursors for each of the eight possible Rydberg orbital symmetries of TMCBD (D_{2h} point group) is listed in Table V. This table makes specific reference to the case where the Rydberg orbitals are cited in LCRO multicenter format. The four bottom lines cite the symmetry species for which the s, p, and d Rydberg AO's, single-centered and located on the inversion center, constitute a basis. Hence, whether the Rydberg orbital is represented in an AO or LCRO form, one can readily enumerate the number of real precursors. It is clear that the s, d_{z^2} and $d_{x^2-y^2}$ Rydberg AO's possess a total of ten precursors and that the numbers for d_{xy}, d_{zx}, d_{yz}, p_x, p_y, and p_z are quite different. In other words, apart from d_{z^2} and $d_{x^2-y^2}$, the atomic relations hold reasonably well. However, there are significant differences in all instances and the effects which these could exert on quantum defect ranges and on the relevance of the empirical s, p, d labeling could certainly be large.

In composite molecules, which can be viewed as a conjunction of two separate and distinct parts, the LCRO model accounts for precursor orthogonality requirements in a quite natural way. Each constituent Rydberg orbital is orthogonal, by construction, to its precursors on its own segment of the molecule. And if the two constituent parts are sufficiently far apart, the orthogonality cross terms (i.e., overlaps) between a Rydberg orbital on one part and its precursors on the other will be quite small. Thus, the values of the quantum defects for the systems A and A_LA_R should exhibit no more than minor variations, whereas transition selection rules could be very different. It is, on the other hand, rather difficult to imagine any one-center description of the Rydberg orbitals of TMCBD (i.e., A_LA_R) which could relate the Rydberg orbitals for acetone to those for TMCBD.

The concept of precursors is conveniently rephrased in the terminology of pseudopotential theory.[30] The Rydberg/precursor orthogonality requirement is simply replaced by an extra potential term. To be specific, the Philips-Kleinmann pseudopotential for TMCBD may be written as a sum[31] of two identical terms, one for each of the two C=O groups. Thus,

$$V^{PK} = V_L{}^{PK} + V_R{}^{PK} \tag{10}$$

The condition for the applicability of an LCRO description

$$\varphi_{LR}{}^{R} = c_1\varphi_L{}^{R} + c_2\varphi_R{}^{R} \tag{11}$$

merely requires that cross terms such as $\langle\varphi_L{}^{R}|V_R{}^{PK}|\varphi_L{}^{R}\rangle$ are all small. The extension of these ideas to polyatomic Rydberg chromophores (e.g., benzene) and the conditions to be imposed in order to retain the concept of s, p, d, . . . labeling in such systems should now be clear.

Unfortunately, our experimental results are less conclusive than we would wish. For example, one might surmise by inspection of Table V that the d_{z^2}, one-center, Rydberg orbital could serve as an attractive candidate for the terminal orbital of the 1860-Å absorption band. One could argue that the large number of precursors to this orbital should cause it to have an extraordinarily small quantum defect; one could also argue that the core charge is heavily localized on two widely separated centers (i.e., the carbonyl groups), that the large d_{z^2} orbital has considerable amplitude at these same centers and that, as a result, this orbital should be stabilized (i.e., exhibit a large term value). Both arguments are persuasive and congruent. However, we tend to reject this possibility for two reasons:

(a) Allowing such abnormal quantum defect values for d Rydbergs would significantly reduce the assignment power invested in δ values.[3a] It may be that this investiture is wrong but, for the moment, it seems unwise to disregard one of the few simple empirical assignment tactics which are available to us.

(b) It is difficult to see why this particular terminal a_g orbital should confer high intensity on the corresponding Rydberg transition when all other transitions to a_g orbitals, particularly the first s, are of very low intensity and when we also can adduce arguments indicating that transitions to a_g terminal orbitals should be weak (vide infra).

The LCRO description, on the other hand, provides a simple alternative. It is true that the LCRO supposition requires further testing. However, we do know of another case where an LCRO description seems mandatory. One of the Rydberg series of *trans*-dibromoethylene[32] which converges on the fourth ionization limit must, on the basis of quantum defect values, be categorized as d. Such a categorization implies, in an atomic Rydberg basis, that the transitions of this series are g → g—this, of course, cannot be correct.

Transition Intensities. Some comment concerning the low intensity of the $b_{2u} \rightarrow a_g$ transitions of TMCBD is required. The a_g Rydberg orbitals possess six *valence* precursors (a_g), four of which are not centered on the carbonyl groups (Table V). In order to maintain the a_g Rydberg/precursor orthogonality, a considerable amount of electron density in the a_g Rydberg orbital must be located some distance from the carbonyl centers. This delocalization will lead to a considerable reduction of transition density. Thus, the Rydberg/precursor orthogonality requirement for the s-type Rydbergs of TMCBD is equivalent to a partial delocalization of the s-type orbitals onto the alkyl substituents. Such a delocalization has been suggested, for other reasons, by Robin.[33]

A similar intensity decrease in R(s) ← N transitions is expected for all heavily methylated ketones and appears to be observed fairly generally.[34] A good example is provided by diisopropyl ketone.[3a]

The LCRO p_y Rydberg orbital of b_{3g} symmetry is the only one to which a transition from the b_{2u} lone-pair orbital is allowed and which, simultaneously, has oxygen lone-pair orbitals as precursors. Thus, it is hardly surprising that the $b_{2u} \rightarrow b_{3g}(1p_y)$ transition is the most intense transition assigned in the TMCBD spectrum.

Concluding Remarks

We have elaborated an LCRO model, one which is implicit in a number of quantum computations,[27,31] and have investigated some of its fundamental properties, particularly those which relate to symmetry. The vacuum uv spectra of acetone and TMCBD have been analyzed in an attempt to decide which of two models—the LCRO model or a one-center model—provides the better description of the Rydberg orbitals of TMCBD. Although the data obtained are not fully conclusive, they do favor the LCRO model quite heavily.

The distinction between the two models, reduced to bare essentials, is based on the following observations: the highest occupied MO of TMCBD is a b_{2u} lone-pair orbital.[10,11] An intense Rydberg transition with $\delta = 1.52$ is observed in TMCBD. This transition appears to be electronically allowed and to necessitate a planar D_{2h} excited-state conformation. Being unwilling, for reasons of quantum defect values, to label this transition as "d-type", we are forced into a "p-type" labeling. Immediately we do so, we are simultaneously forced, in order to account for the apparent dipole allowedness of this transition, to use an LCRO prescription.

Acetone/TMCBD is not the perfect dyad on which to test the ideas contained in this work. It would have been nice to avoid the ring strain inherent to TMCBD and to eliminate the need for methyl substituents. Nonetheless, we believe that we have provided a means by which chemical relatedness can be transcribed onto Rydberg spectra and that we have advanced considerable justification for it.

The prime purpose of our work has been to relate the very useful quantum defect concept to ideas which are more chemical in nature. While we may not have been totally successful in this effort, we have suggested an approach, partially proven the viability of this approach, and provided relevant guidelines for further work along these same lines.

References and Notes

(1) This work was supported by the U.S. Energy Research and Development Administration, Division of Biomedical and Environmental Research, Physics and Technological Program, and by the Deutsche Forschungsgemeinschaft via an Ausbildungsstipendium.

(2) J. W. Rabalais, "Photoelectron Spectroscopy", Wiley-Interscience, New York, N.Y., 1976; H. Bock and B. G. Ramsey, *Angew. Chem.*, **85**, 773 (1973) [*Angew. Chem., Int. Ed. Engl.*, **12**, 734 (1973)]; C. R. Brundle and M. B. Robin in "Determination of Organic Structures by Physical Methods", F. C. Nachod and J. J. Zuckerman, Ed., Academic Press, New York, N.Y., 1971.

(3) (a) M. B. Robin, "Higher Excited States of Molecules", Vol. I and II, Academic Press, New York, N.Y., 1974/75; (b) P. Hochmann, P. H. Templet, H.-t. Wang, and S. P. McGlynn, *J. Chem. Phys.*, **62**, 2588 (1975).

(4) See ref 3a, Vol. I, pp 22, 44.

(5) W. H. E. Schwarz, *Chem. Phys. Lett.*, **9**, 157 (1975).
(6) For a fuller discussion, with citations, see ref 3a above.
(7) R. S. Mulliken, *J. Am. Chem. Soc.*, **86**, 3183 (1964).
(8) A. Sommerfeld, "Atombau und Spektrallinien", Vol. II, F. Vieweg and Sohn, Braunschweig, 1953, p 140.
(9) G. Herzberg and C. Jungen, *J. Mol. Spectrosc.*, **41**, 425 (1972).
(10) D. O. Cowan, R. Gleiter, J. A. Hashmall, E. Heilbronner, and V. Hornung, *Angew. Chem.*, **83**, 405 (1971) [*Angew. Chem., Int. Ed. Engl.*, **10**, 401 (1971)].
(11) P. Brint, D. R. Dougherty, and S. P. McGlynn, *Photochem. Photobiol.*, in press.
(12) See, for example, H. Hosoya, *Int. J. Quantum Chem.*, **6**, 801 (1972); or A. D. Liehr, *Z. Naturforsch. A*, **11**, 752 (1956).
(13) C. R. Brundle, M. B. Robin, N. A. Kuebler, and M. Basch, *J. Am. Chem. Soc.*, **94**, 1451 (1972).
(14) For Raman and ir of various phases, and normal coordinate analyses, see F. O. Nicolaisen, O. F. Nielsen, and M. Vala, *J. Mol. Struct.*, **13**, 349 (1972).
(15) For x-ray diffraction data, see P. H. Freidlander, T. H. Goodwin, and J. M. Robertson, *J. Chem. Soc.*, 3080 (1956); C. Riche, *C. R. Acad. Sci.*, **245**, 543 (1972); C. D. Shirrell and D. E. Williams, *Acta Crystallogr., Sect. B*, **30**, 245 (1974). For electron diffraction data, see W. N. Lipscomb and V. Shomaker, *J. Chem. Phys.*, **14**, 475 (1946).
(16) D. A. Ramsey in "Determination of Organic Structure by Physical Methods", Vol. 2, F. C. Nachod and W. D. Phillips, Ed., Academic Press, New York, N.Y., 1962.
(17) M. Vala, *J. Am. Chem. Soc.*, in press.
(18) P. Brint and S. P. McGlynn, *J. Am. Chem. Soc.*, in press.
(19) N. J. Turro, P. A. Leermakers, H. R. Wilson, D. C. Neckers, G. W. Byers, and G. E. Vesley, *J. Am. Chem. Soc.*, **87**, 2613 (1965).
(20) R. H. Huebner, R. J. Celotta, S. R. Mielczarek, and C. E. Kuyatt, *J. Chem. Phys.*, **59**, 5434 (1973).
(21) K. Watanabe, *J. Chem. Phys.*, **22**, 1564 (1954).
(22) A. B. F. Duncan, *J. Chem. Phys.*, **3**, 131 (1935).
(23) E. Lindholm, *Ark. Fys.*, **40**, 97 (1969).
(24) References in G. Herzberg, "Electronic Spectra and Electronic Structure of Polyatomic Molecules", Van Nostrand, New York, N.Y., 1966, p 658.
(25) R. E. Ballard and C. H. Park, *Spectrochim. Acta, Part A*, **26**, 43 (1970).
(26) M. Vala, I. Trabjerg, and E. N. Svendsen, *Acta Chem. Scand., Ser. A*, **28**, 37 (1974).
(27) Molecular computations, for example those of Fischer-Hjalmars and Kowalewski [I. Fischer-Hjalmars and J. Kowalewski, *Theor. Chim. Acta*, **27**, 197 (1972)], are available in which the basis set consisted of diffuse orbitals on various atomic centers. Implicity, of course, this is an LCRO model. However, in order to achieve reasonable reliability in the calculated energies, extended basis sets and extensive configuration interaction usually are required. As a result, the question of the best zero-order description is somewhat a question of numerics and/or machine costs.
(28) W. H. E. Schwarz, *Chem. Phys.*, **9**, 157 (1975).
(29) See ref 3a, Vol. I, p 51.
(30) J. D. Weeks, A. U. Hazi, and S. A. Rice, *Adv. Chem. Phys.*, **16**, 283 (1969); A. U. Hazi and S. A. Rice, *J. Chem. Phys.*, **48**, 495 (1968).
(31) See, for example, the treatment of O_2 and C_2H_4 by T. Betts and V. McKoy, *J. Chem. Phys.*, **54**, 113 (1971).
(32) K. Wittel, W. S. Felps, and S. P. McGlynn, *J. Chem. Phys.*, submitted for publication.
(33) See ref 3a, Vol. I, pp 56, 57, and M. B. Robin, *Int. J. Quantum Chem.*, **6**, S257 (1972).
(34) W. C. Tam and C. E. Brion, *J. Electron Spectrosc. Relat. Phenom.*, **4**, 139 (1974).

Coupled Hartree–Fock Calculations of Nuclear Magnetic Resonance Carbon–Carbon Coupling Constants in Substituted Benzenes

Paolo Lazzeretti,* Ferdinando Taddei, and Riccardo Zanasi

Contribution from Istituto di Chimica Organica, Università, 41100 Modena, Italy.
Received November 26, 1975

Abstract: The coupled Hartree–Fock perturbation theory is applied, within the limits of INDO approximation, to compute direct and long-range coupling constants between ^{13}C nuclei in substituted benzenes. Contact, orbital, and dipolar terms are used throughout the calculations, showing that the Fermi contact is often insufficient to account for the observed couplings. Agreement with experimental data is quite satisfactory and much better than with other calculations. A preliminary determination of the parameters necessary in the semiempirical calculation afforded the values $s_C^2(0)s_C^2(0) = 13.5150$ au, $\langle r^{-3}\rangle_C\langle r^{-3}\rangle_C = 7.9832$ au.

The theory of nuclear spin–spin coupling has its roots in the pioneering work of Ramsey,[1,2] who showed that three distinct mechanisms concur in determining this interaction, namely the Fermi contact term, nucleus–nucleus dipolar interaction, and nuclear spin–electron orbit coupling. Ramsey tackled the problem of computing coupling constants measured in NMR spectroscopy by means of the conventional perturbation theory. Because of difficulties encountered in handling the second-order perturbation formula, McConnell introduced the closure approximation,[3] using an average excitation energy in his MOLCAO approach. Some authors, however, suggested that the use of mean energy approximation is far from valid, the convergence of the perturbation expansion needing to be carefully checked.[4,5] A refined MOLCAO procedure was introduced by Pople and Santry[6] which, by overcoming the average excitation energy approximation, provides improved results.

A more promising method was recently proposed by Pople et al.;[7] they put forward a "finite perturbation theory" (FPT) using a variational wave function which contained the perturbation explicitly. Nevertheless, the Hartree–Fock perturbation theory seems to provide more flexible and powerful methods of computing nuclear spin coupling constants: the coupled Hartree–Fock perturbation theory (CHFPT)[8] has been used to calculate the contact interaction by Power and Pitzer;[9] Blizzard and Santry[10] have evaluated the contributions of all three mechanisms studied by Ramsey allowing for the INDO approximation.[11] Ab initio calculations by Ditchfield and Snyder[12] are also available. These authors[10] show that dipolar and orbital terms are far from negligible in C–C, C–F, and F–F couplings.

In the present paper, CHFPT is applied to compute carbon–carbon coupling constants in substituted benzenes. Fermi contact, orbital, and dipolar terms are taken into account within the framework of INDO approximation. Some preliminary work is devoted to evaluating an empirical set of parameters to be used in the actual calculations: the necessary quantities are the electron density at carbon nucleus, $s_C^2(0)$, and the mean value $\langle r^{-3}\rangle_C$.

Outline of Calculation

The computational scheme employed is essentially the same as that used to evaluate electric polarizabilities and magnetic susceptibilities,[13] hence only master equations are referred to